Available online at www.sciencedirect.com

ScienceDirect

Ceramics International 40 (2014) 4599–4605

CERAMICS INTERNATIONAL

www.elsevier.com/locate/ceramint

Mechanism of Fe_2TiO_5 as oxygen carrier for chemical looping process and evaluation for hydrogen generation

Young Ku[a,*], Yu-Cheng Liu[a], Ping-Chin Chiu[a], Yu-Lin Kuo[b], Yao-Hsuan Tseng[a]

[a]Department of Chemical Engineering, National Taiwan University of Science and Technology, Taipei 10607, Taiwan
[b]Department of Mechanical Engineering, National Taiwan University of Science and Technology, Taipei 10607, Taiwan

Received 13 June 2013; received in revised form 12 August 2013; accepted 31 August 2013
Available online 6 September 2013

Abstract

Fe_2TiO_5 was studied for the reduction mechanism in chemical looping process. Fe_2TiO_5 pellets were reduced by syngas that demonstrated highest reduction rate in the beginning of reduction period from Fe_2TiO_5 to $FeTiO_3$ and Fe_2TiO_4. The reduction of Fe_2TiO_5 is suggested in sequence from Fe_2TiO_4, $FeTiO_3$ to Fe. Fe_2TiO_5 pellets performed reasonable reactivity and steady recyclability after continuous 100 redox cycles. The increased surface area and decreased mechanical strength for pellets operated after 30 redox cycles was due to formation of cracks and porous structures. Moreover, Fe_2O_3/TiO_2 was the major crystalline phase existed in the pellets after 30 redox cycles. Fe_2TiO_5 attributed high syngas conversion in the fixed bed reactor due to high equilibrium constants. The completed reduced form of Fe_2TiO_5 oxygen carriers, Fe/TiO_2, demonstrated hydrogen generation by steam oxidation, and the Fe was oxidized to Fe_3O_4 and $FeTiO_3$ in the fixed bed reactor.

Keywords: Chemical looping; Fe_2TiO_5; Oxygen carrier; Hydrogen generation

1. Introduction

Chemical looping technology was proposed to increase combustion efficiency of fuels as well as inherently to generate high purity CO_2 [1]. Oxygen carrier is the looping media to provide oxygen for fuel combustion, and the reduced oxygen carrier is oxidized to the fully oxidation state for successive redox cycles [2]. A chemical looping system comprises a fuel reactor and an air reactor for continuous reduction and oxidation of oxygen carriers, respectively, as illustrated in Fig. 1 [3]. In the fuel reactor, oxygen carriers release oxygen for fuel combustion, and CO_2 with over 90% purity is yielded after H_2O condensation. The reduced oxygen carriers are then moved to the air reactor by mechanical devices, such as loop seal, valves and air compressor [4]. The oxidation of reduced oxygen carriers is carried out in the air reactor for heat generation.

Oxygen carriers should provide with high reaction rate, high oxygen carrying capacity, great mechanical strength, and long-term recyclability for applications of chemical looping process [5]. Ni-, Fe-, Cu-, Mn- and Co-based metal oxides are the typical materials validated by thremogravimetric analysis (TGA) to be employed as oxygen carriers [6,7]. However, their reactivity and recyclability are greatly reduced due to the sintering and attrition of oxygen carriers during the chemical looping operation. Therefore, through coupling support materials, such as SiO_2, Al_2O_3, TiO_2, MgO, ZrO_2, with the validated metal oxides to manufacture oxygen carrier was an effective way to avoid sintering and to reinforce the mechanical strength of oxygen carriers [8,9]. However, the application of massive fabricated oxygen carriers may significantly boost the operational cost of chemical looping process. Therefore, the application of low-cost natural minerals as oxygen carriers, such as ilmenite, was frequently studied for chemical looping process [10].

The feasibility of application of ilmenite as oxygen carrier has been widely evaluated with various fuels, such as syngas, methane, coal and petroleum coke in recent years [11–13]. Combustions of methane and syngas (H_2 and CO) with ilmenite were investigated by a lab-scale fluidized bed reactor [14] and a 120 kW circulating fluidized bed reactor [15], both literatures indicated that over 80% of CO conversion was achieved for experiments conducted at temperature above 960 °C; however, only around 40% of CH_4 conversion was achieved under similar operating condition. For coal and petroleum coke combustions,

*Corresponding author. Tel.: +886 2 23785535; fax: +886 2 27376644.
E-mail address: ku508@mail.ntust.edu.tw (Y. Ku).

0272-8842/$ - see front matter © 2013 Elsevier Ltd and Techna Group S.r.l. All rights reserved.
http://dx.doi.org/10.1016/j.ceramint.2013.08.138

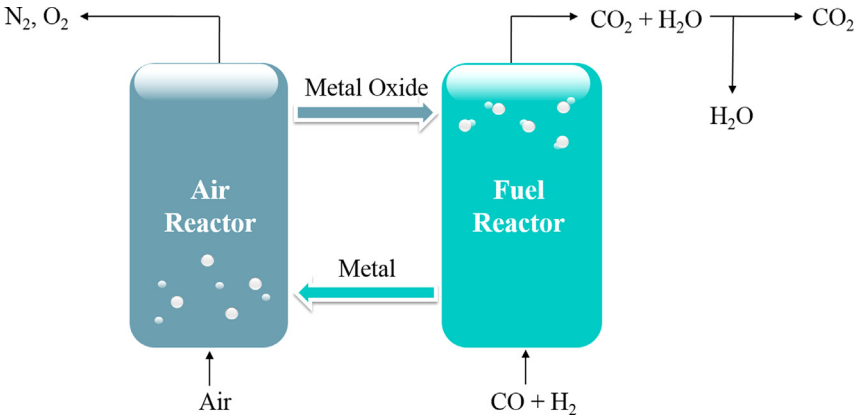

Fig. 1. Scheme of chemical looping process.

ilmenite showed relatively satisfactory combustion efficiency with $Fe_2O_3/MgAl_2O_4$ composite oxygen carriers in a laboratory scale fluidized-bed reactor operated at 950 °C [16]. Ilmenite demonstrated similar performance to the fabricated iron-based oxygen carriers; therefore, ilmenite was frequently selected for solid fuel combustion in sub-pilot scale fluidized bed reactors [17,18].

In order to investigate the mechanism of ilmenite for chemical looping operation, Fe_2TiO_5, as the fully oxidation state of ilmenite [14], was selected as oxygen carrier in this study. The redox cycles were conducted by thermogravimetrirc analyzer (TGA), and the crystalline phases and surface morphology of the Fe_2TiO_5 pellets during the redox cycling were identified by X-ray diffraction (XRD) and field-emission scanning electron microscope (FESEM), respectively. The analysis of effluent gas during the reduction and oxidation of Fe_2TiO_5 were conducted using a fixed bed reactor. Experiments with regard to steam oxidation with completely reduced Fe_2TiO_5 pellets for H_2 generation in a fixed-bed reactor, and the crystalline phases of oxygen carriers were identified by XRD patterns.

2. Experimental

Cylindrical Fe_2TiO_5 pellets (10 mm in diameter and 2 mm in height) for thermogravimetric and X-ray diffraction analysis were made of Fe_2TiO_5 (99.9%, Alfa Aesar) powder after ball-milled, and were prepared by single-punch tablet press. 200 mg of Fe_2TiO_5 pellets were loaded in an alumina crucible for TGA analysis using a Netzsch STA 449F3 analyzer, the temperature of TGA chamber was raised with a ramping rate of 20 °C/min in N_2 atmosphere, and eventually kept at 900 °C. 200 mL/min reducing gas composed of 10% H_2, 10% CO and 80% N_2 was introduced into TGA chamber for 140 min to reduce Fe_2TiO_5. After the reduction phase, 200 mL/min N_2 was introduced for 20 min for sweeping reducing gas contained in the TGA chamber. 200 mL/min air was then introduced for 30 min to oxidize the reduced oxygen carriers. The conversion for oxygen carriers (X_{oc}) is defined as:

$$X_{OC} = \frac{m(t) - m_r}{m_o - m_r} \quad (1)$$

where m_o is the weight of fully oxidized oxygen carriers; m_r is the weight of fully reduced oxygen carriers; $m(t)$ is the weight of oxygen carriers after reduction period of t. For determining the conversion of oxygen for Fe_2TiO_5, only three oxygen atoms were counted for fully oxidized oxygen carriers because other two oxygen atoms were contributed to TiO_2 as the support material. The reduction and oxidation was replicated for 100 cycles to determine the reactivity and recyclability of the prepared Fe_2TiO_5 pellets; the periods of reduction, purging and oxidation phases were 10, 5 and 6 min, respectively.

Fixed bed reactor system employed in this study is shown in Fig. 2, and is composed of a 25.4 mm ID stainless steel (SS310) reactor and a PID-controlled heating element covering 200 mm of reactor height. A plate with sixteen 0.25 mm apertures was located in the lower part of the reactor for supporting 1 g of Fe_2TiO_5 pellets. Fe_2TiO_5 pellets were reduced at 900 °C, by introducing 200 mL/min reducing gas composed of 10% CH_4, 10% H_2 and 80% N_2 into the reactor. N_2 gas was then purged into the fixed bed reactor to sweep out the residual reducing gas prior to subsequent oxidization phase. Steam generated by the pre-heat element was injected into the reactor for H_2 generation with the rate of 2.64 mol/min controlled by a syringe pump (KDS-100).The outlet stream from the fixed bed reactor was passed through a cold trap to condense steam, and was consequently analyzed by a non-dispersive infrared analyzer (Molecular Analysis 6000i) to detect the concentration of CO and CO_2. A gas chromatography analyzer equipped with thermal conductivity detector (Agilent 7890) was used for measuring H_2 concentration. The phase transformation of Fe_2TiO_5 during redox cycling was characterized by the X-ray diffractometer (XRD, Bruker D2 Phaser), the incident beam was Cu K_α characteristic X-ray at 30 kV and 10 mA, and employing a scanning rate of 0.05° s^{-1} in the 2θ range from 10° to 80°. Surface morphology and interfacial behaviors of Fe_2TiO_5 pellets were analyzed with field emission scanning electron microscope (FESEM, JOEL JSM-6500F). The surface area of Fe_2TiO_5 pellets was determined by a Brunauer Emmett Teller (BET) analyzer (MICROMETRICS, ASAP 2020) using N_2 as adsorption media.

3. Results and discussion

The temporal conversion of Fe_2TiO_5 pellets reduced by syngas for 140 min and oxidized by air for 20 min in TGA is illustrated in Fig. 3, indicating that the reduction of Fe_2TiO_5

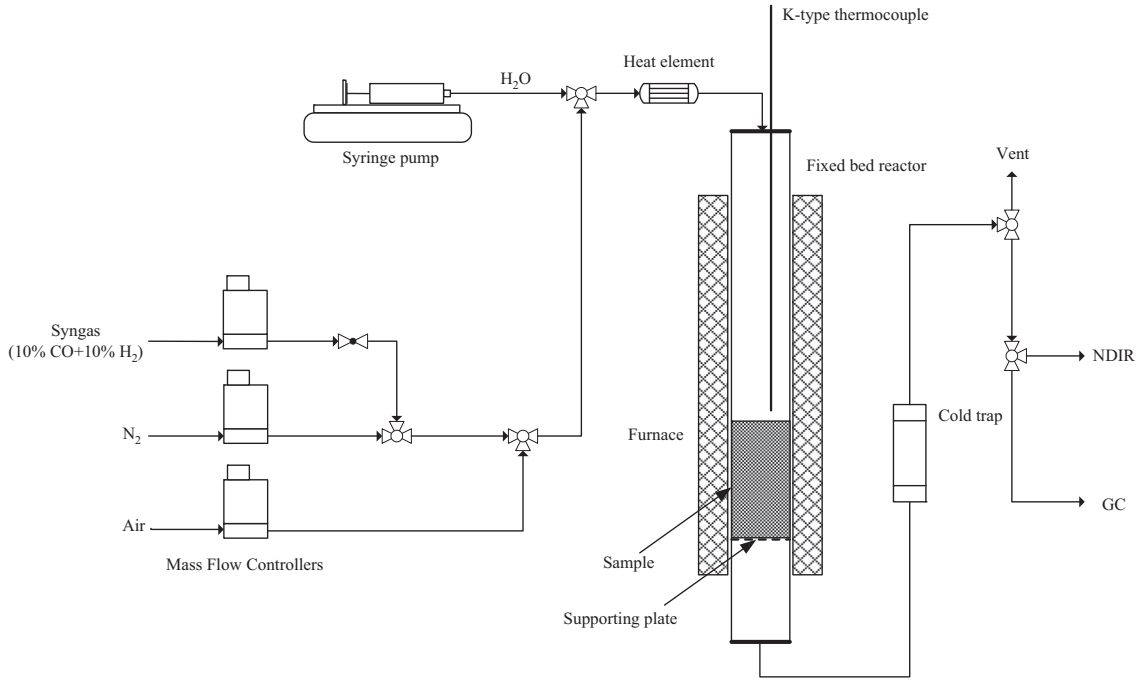

Fig. 2. Scheme of fixed bed reactor system.

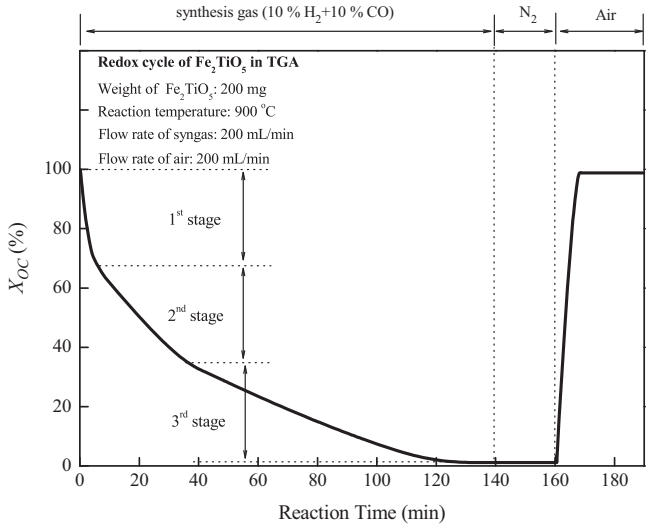

Fig. 3. Degree of conversion as a function of reaction time for single redox cycle of Fe_2TiO_5 conducted with 200 mL/min of syngas for reduction and 200 mL/min of air for oxidation at 900 °C.

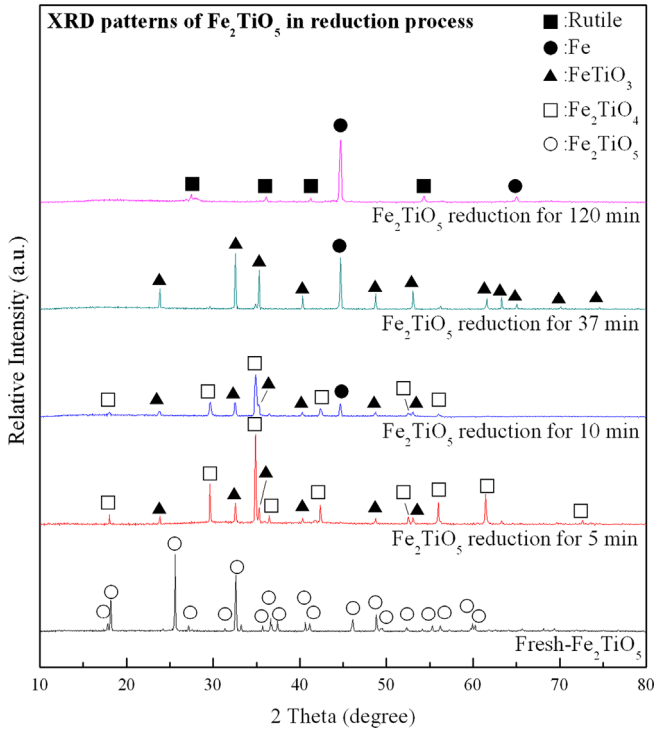

Fig. 4. XRD patterns of Fe_2TiO_5 fresh pellet, and the pellets sampled at 5, 10, 37 and 120 min in the reduction phase conducted by TGA at 900 °C.

pellets can be roughly divided into 3 consecutive stages. In the first stage, 30 wt% of oxygen contained in Fe_2TiO_5 was rapidly reduced in 5 min. From 5 to 37 min for the second stage, the reduction rate was decreased and approximately 40 wt% of oxygen was reduced. Finally, the remaining 30 wt% of oxygen was reduced from 37 to 140 min for the third stage. The pellets were then sampled at the reduction time of 5, 10, 37 and 120 min for phase characterization by XRD, the results are shown in Fig. 4, Fe_2TiO_5 was the sole crystalline phase of the fresh pellet. After 5 min of reduction, $FeTiO_3$ and Fe_2TiO_4 were found to be the major crystalline phases. Therefore, the reduction of Fe_2TiO_5 pellets in the first stage is suggested by following reactions:

$$2Fe_2TiO_5 + H_2 + CO \rightarrow 2Fe_2TiO_4 + H_2O + CO_2 \quad (2)$$

$$2Fe_2TiO_4 + 2TiO_2 + H_2 + CO \rightarrow 4FeTiO_3 + H_2O + CO_2 \quad (3)$$

For pellets sampled at 10 min of reduction, Fe was observed and the intensity of Fe_2TiO_4 was decreased. For pellets

sampled at 37 min of reduction, Fe and $FeTiO_3$ were observed to be the major crystalline phases, while Fe_2TiO_4 was almost vanished in the XRD pattern. Hence, reactions (3) and (4) are suggested taken place in the second stage.

$$2FeTiO_3 + H_2 + CO \rightarrow 2Fe + 2TiO_2 + H_2O + CO_2 \quad (4)$$

For pellets sampled at 120 min of reduction, only Fe and TiO_2 were identified indicating that $FeTiO_3$ was complete reduced. Therefore, sequential stages of reduction may restrain the overall reactivity of iron-based oxygen carriers; only the oxygen reduced in the first stage would be utilized for most studies [14,19]. Furthermore, Fe_2TiO_4 and $FeTiO_3$ generated during reduction might serve as support materials as well as oxygen carriers for chemical looping process.

Fe_2TiO_5 pellets were examined in TGA for continuous 100 redox cycles with 5 minutes for each redox cycle. The utilization of oxygen was maintained at approximately 33% during 100 continuous redox cycles operated at 900 °C, shown in Fig. 5, indicating that Fe_2TiO_5 pellets exhibited reasonable reactivity and steady recyclability as oxygen carriers. Fe_2TiO_5 pellets were sampled at 1, 30 and 100 redox cycles, and were characterized by XRD. As shown in Fig. 6, for Fe_2TiO_5 pellets operated after 30 redox cycles, Fe_2O_3 and TiO_2 were the major crystalline phases indicating that Fe_2TiO_5 was reformed as Fe_2O_3/TiO_2 composite. The crystalline phase of pellets was still Fe_2O_3/TiO_2 composite after 100 redox cycles; therefore, Fe_2O_3/TiO_2 composite was the full oxidation state for continuous redox cycling. Hence, reaction (2) was modified as reaction (5).

$$2Fe_2O_3 + 2TiO_2 + H_2 + CO \rightarrow 2Fe_2TiO_4 + H_2O + CO_2 \quad (5)$$

The surface morphology of fresh Fe_2TiO_5 pellets, and the pellets operated after 1, 30 and 100 redox cycles were observed by SEM with 100× of magnification. As shown in Fig. 7(a) and (b), the surfaces of fresh pellets and pellets operated after only one redox cycle were observed to be very condensed. However, cracks and porous structures were found on the surface of pellets operated after 30 redox cycles, as revealed in Fig. 7(c) and (d), leading to the increase of BET surface area

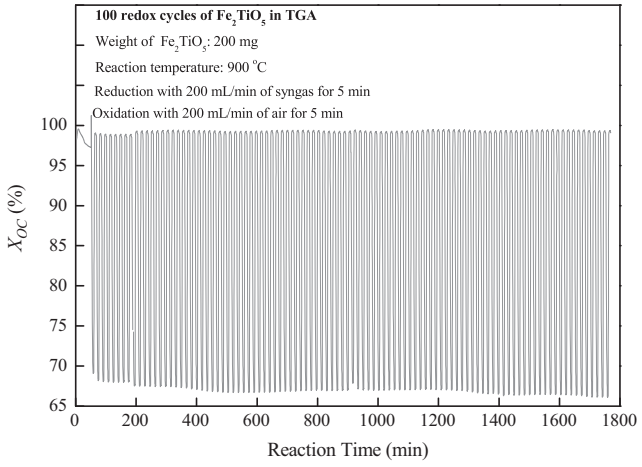

Fig. 5. Degree of conversion as a function of reaction time for Fe_2TiO_5 pellets during the 100 redox cycles at 900 °C.

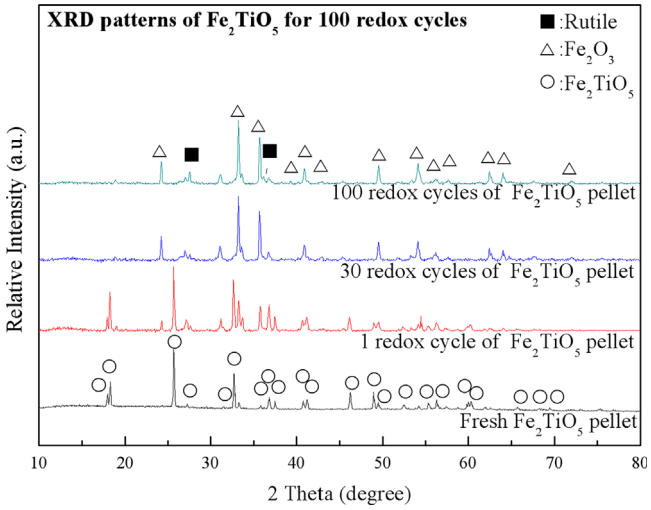

Fig. 6. XRD patterns of Fe_2TiO_5 pellets for fresh pellets, and the pellets operated after 1, 30 and 100 redox cycles at 900 °C.

from 0.75 m^2/g for fresh pellets to 1.16 m^2/g for pellets operated after 100 redox cycles. Similar observations of porous structure for titanium supported Fe_2O_3, which leading to better reactivity, were reported in the previous studies [14,19]. Li et al. reported that interaction between Fe ions and TiO_2 resulted in lattice substitution during redox cycling, since the size of Fe ions are similar with Ti ions. The observations by SEM and EDX illustrated Fe ions were moving toward the surface to form condensed surface and left porous structure in the inner side of particle [20]. Fe_2TiO_5 pellet prepared in this study illustrated similar phenomena observed after 30 redox cycles as well as demonstrated better reactivity. The cracks were found by the previous study for synthetic Fe_2TiO_5 oxygen carriers during the redox cycles in a fluidzied bed reactor; however, no obvious cracks were found for natural ilmentite [21]. The species present in natural ilmenite, such as SiO_2, CaO, MgO, Al_2O_3, MnO [12], may enhance the mechanical strength of ilmenite. By observing 5000× SEM images, the size of grain was enhancing with increasing operated redox cycles as shown in Fig. 7(e)–(h). The size of grains on the surface of fresh pellets was observed to be roughly 0.5–10 μm, as shown in Fig. 7(e). Grains on the surface of pellets were sintered after the first redox cycle as observed in Fig. 7(f), which was corresponded to the observation of iron-based oxygen carriers reported by the literature [22]. However, the 100× SEM image of pellets after the first redox cycle did not illustrate noticeable change comparing with fresh pellets, as revealed in Fig. 7(b). Agglomeration of grains on the pellets was more noticeable operated after 30 and 100 redox cycles as shown in Fig. 7(g) and (h). The increase of grain size is probably provoked by the agglomeration of Fe_2O_3 because Fe_2O_3 is identified to be the major crystalline phase by XRD for pellets operated for redox cycles. Based on the experience of ceramic sintering, the occurrence of solid state sintering for ceramic materials would be started at around 2/3 of its melting point [23]. The 900 °C of operating temperature employed in this study was closed to 2/3 of melting point of Fe_2O_3 (1560 °C) and Fe (1535 °C); therefore, the grain size of Fe_2O_3 was increased possibly because of the solid state

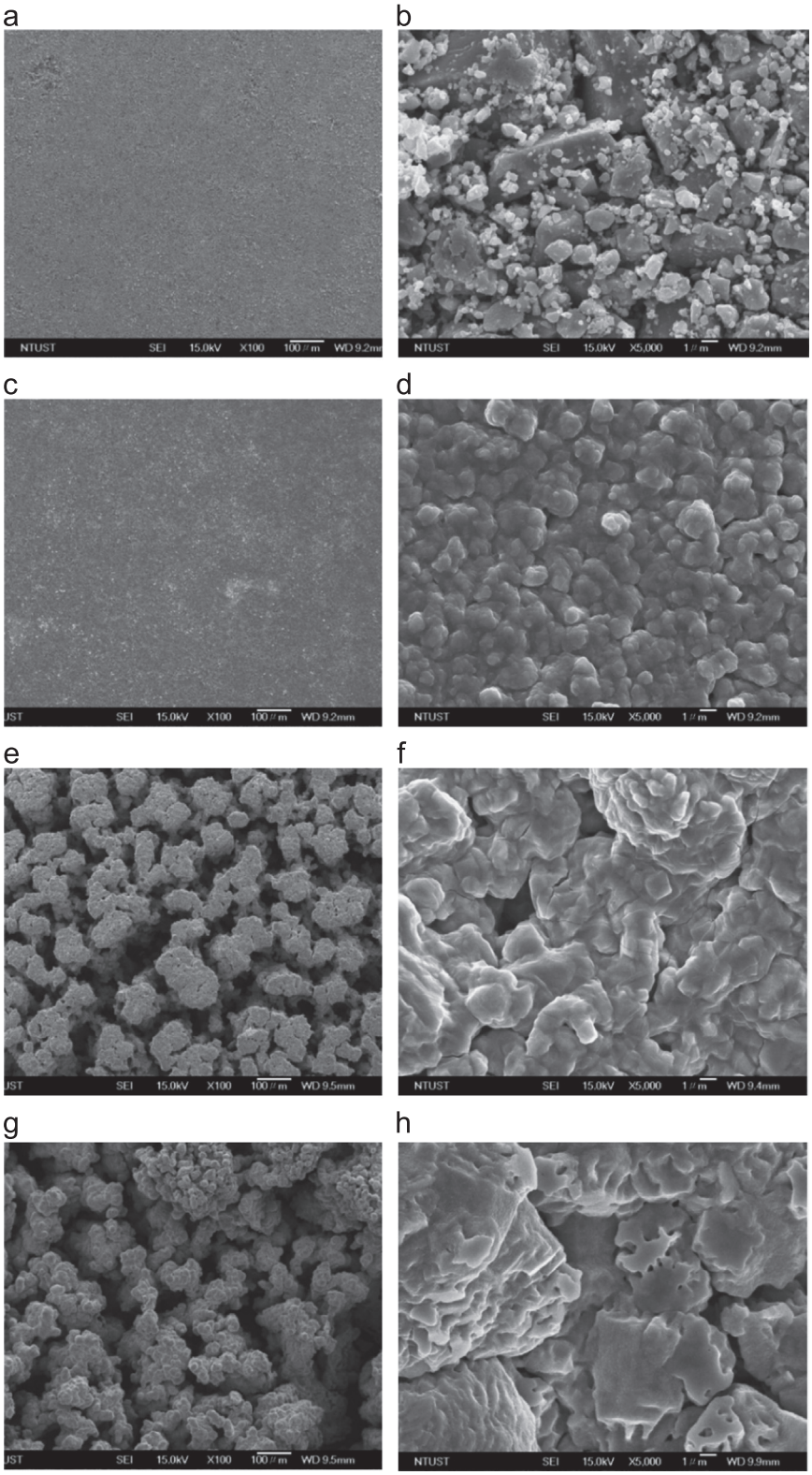

Fig. 7. SEM images of 100x Fe_2TiO_5 pellets for (a) fresh pellets, operated after (b) 1 redox cycle, (c) 30 redox cycles and (d) 100 redox cycles; 5000x Fe_2TiO_5 pellets for (e) fresh pellets, operated after (f) 1 redox cycle, (g) 30 redox cycles and (h) 100 redox cycles at 900 °C.

sintering during redox cycling. Consequently, the formation of cracks may improve the reactivity of oxygen carriers by increasing the surface area, since the grain size of Fe_2O_3 was increased.

Combustion of syngas with Fe_2TiO_5 pellets was employed in a fixed bed reactor at 900 °C as shown in Fig. 8. Only CO_2 was detected in the outlet stream during the time between 80 and 100 s indicating complete combustion of syngas was

achieved. The high CO_2 yields for the reduction of Fe_2TiO_5 by syngas, as described by reactions (2) and (3), might be attributed to the very high equilibrium constants of P_{CO_2}/P_{CO} and P_{H_2O}/P_{H_2} for the reduction of Fe_2O_3 by syngas, both around 10^5 [24]. Concentration of CO_2 in the outlet stream was decreased rapidly during the time between 100 and 500 s, while concentrations of CO and H_2 were both increased in this period. The low levels of CO_2 was generated by the reduction of $FeTiO_3$ to Fe with syngas, as depicted by reaction (4), and the equilibrium constants of P_{CO_2}/P_{CO} and P_{H_2O}/P_{H_2} were determined to be between 10^{-1} and 10^1 [24]. The reduction of oxygen carriers was almost completed as CO_2 concentration in the effluent stream approached zero. After N_2 purging, oxidation of iron was then carried out by purging air into the fixed bed reactor from 6100 to 9600 s as described by reaction (6).

$$4Fe + 3O_2 \rightarrow 2Fe_2O_3 \quad (6)$$

CO and CO_2 were observed at the early stage of oxidation indicating that some carbon may be deposited during reduction through Boudard reaction described as follow:

$$2CO \rightarrow CO_2 + C \quad (7)$$

The deposited carbon was then oxidized to form CO and CO_2.

Iron-based oxygen carriers can be employed in reduced form to generate hydrogen by water splitting reaction as described by reactions (8) and (9) [24]:

$$3Fe + 4H_2O \rightarrow Fe_3O_4 + 4H_2 \quad (8)$$

$$3FeO + 3H_2O \rightarrow Fe_3O_4 + 3H_2 \quad (9)$$

The Fe_2TiO_5 pellets were fully reduced to Fe/TiO_2 pellets, as described in sequence of reactions (2)–(4), prior to the introduction of steam to the fixed bed reactor at 900 °C for hydrogen generation. As shown in Fig. 9, steady hydrogen generation was achieved for replicated 5 cycles for experiments with the same stock of pellets. Fe_3O_4 and $FeTiO_3$ were characterized by XRD as shown in Fig. 10 for oxygen carriers

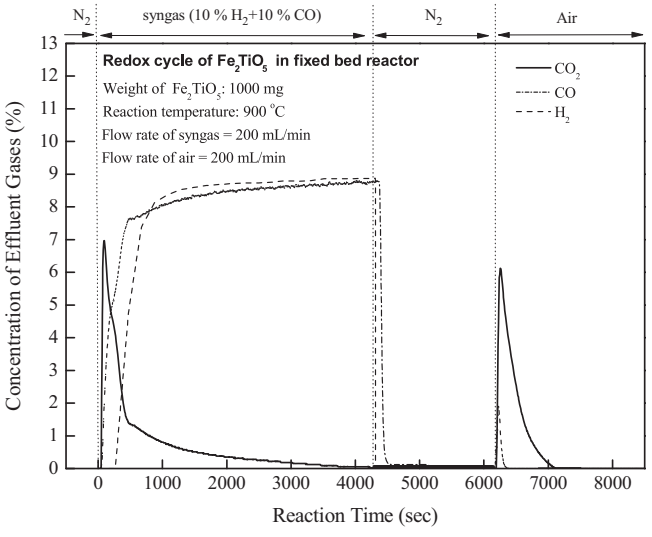

Fig. 8. Concentrations of effluent gases as a function of reaction time for reduction and oxidation of Fe_2TiO_5 pellets from the fixed bed reactor at 900 °C.

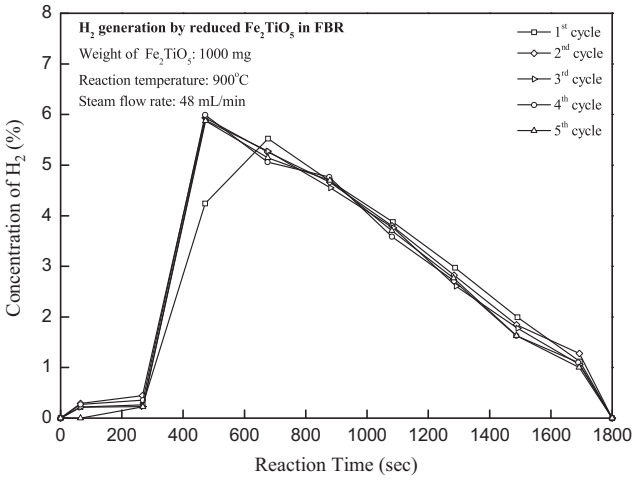

Fig. 9. Concentration of H_2 as a function of reaction time by steam oxidation of full reduced Fe_2TiO_5 pellets replicated for 5 times at 900 °C.

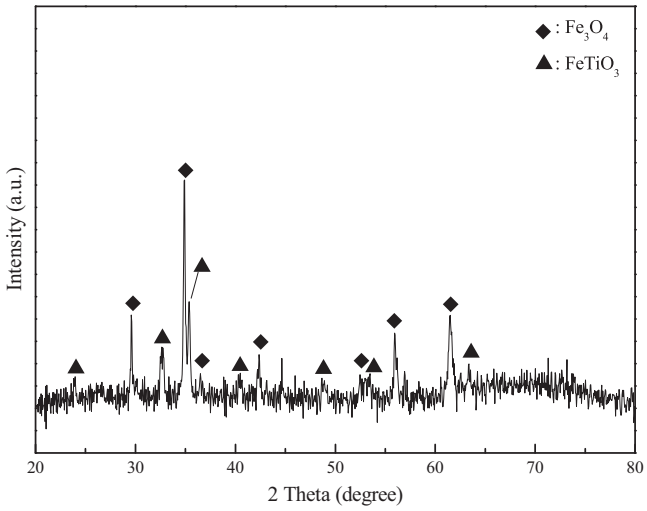

Fig. 10. XRD pattern of the pellet sampled after steam oxidation for H_2 generation at 900 °C.

sampled after steam oxidation. Hence, hydrogen generation through steam oxidation of Fe/TiO_2 pellets can be expressed by reactions (8) and (10).

$$Fe + TiO_2 + 2H_2O \rightarrow FeTiO_3 + H_2 \quad (10)$$

Hence, Fe_2TiO_5 pellets for chemical looping hydrogen generation is suggested employed with counter-flow moving bed reactor, which may provide long residence time for complete reduction of Fe_2TiO_5 to Fe/TiO_2 [25,26].

4. Conclusions

Fe_2TiO_5 pellets which pelletized by commercial Fe_2TiO_5 powders exhibit reasonable reactivity and steady recyclability for experiments conducted by TGA at 900 °C for continuous 100 redox cycles. Three consecutive stages of reduction were illustrated by XRD characterization for the reduction of Fe_2TiO_5 pellets that Fe_2TiO_5 was reduced to $FeTiO_3$ and Fe_2TiO_4 after first stage of reduction; and then Fe and $FeTiO_3$

were observed after the second stage; finally, $FeTiO_3$ was completely reduced to Fe and TiO_2 at the end of reduction. Fe_2O_3/TiO_2 composite was observed to be the full oxidation state of the prepared oxygen carriers instead of Fe_2TiO_5 after 30 redox cycles. The increased grain size of Fe_2O_3 was observed by 5,000x SEM images possibly due to the agglomeration of Fe_2O_3 during redox cycling. However, cracks and porous structures were found on the surface of pellets operated after 30 redox cycles to increase the surface area for reasonable reactivity. Fe_2TiO_5 illustrated high CO_2 yield for syngas reduction in the fixed bed reactor; however, the intermediate phase, $FeTiO_3$, performed low CO_2 yield due to low equilibrium constants for syngas conversion. Hydrogen generation is technically feasible by conducting steam oxidation with Fe/TiO_2 pellets in the fixed bed reactor; however, Fe/TiO_2 was oxidized to Fe_3O_4 and $FeTiO_3$ after steam oxidation. In sum, Fe_2TiO_5 pellet is feasible to be an oxygen carrier for syngas combustion as well as employment of chemical looping hydrogen generation.

Acknowledgment

This research was supported by Grant NSC-98–3114-E-007–013 and NSC- 100–3113-E-007-005 from National Science and Technology Program-Energy in Taiwan.

References

[1] H.J. Richter, K.F. Knoche, Reversibility of combustion processes in efficiency and costing: second law analysis of processes, ACS Symposium Series 235 (1983) 71–85.
[2] M. Ishida, D. Zheng, T. Akehata, A new advanced power generation system using chemical-looping combustion, Energy 12 (1987) 147–154.
[3] T. Mattisson, A. Lyngfelt, P. Cho, The use of iron oxide as an oxygen carrier in chemical looping combustion of methane with inherent separation of CO_2, Fuel 80 (2001) 1953–1962.
[4] L.S. Fan, Chemical Looping Systems for Fossil Energy Conversions, John Wiley & Sons, Inc., Hoboken, New Jersey, 63–66.
[5] M.M. Hossain, H.I. de Lasa, Chemical-looping combustion (CLC) for inherent CO_2 separations-a review, Chemical Engineering Science 60 (2008) 4433–4451.
[6] T. Mattisson, A. Järdnäs, A. Lyngfelt, Reactivity of some metal oxides supported on alumina with alternating methane and oxygen-application for chemical-looping combustion, Energy and Fuels 17 (2003) 643–651.
[7] Q. Zafar, T. Mattisson, B. Gevert, Redox investigation of some oxides of transition-state metals Ni, Cu, Fe, and Mn supported on SiO_2 and $MgAl_2O_4$, Energy and Fuels 20 (2006) 34–44.
[8] T. Mattisson, M. Johansson, A. Lyngfelt, The use of NiO as an oxygen carrier in chemical-looping combustion, Fuel 85 (2006) 736–747.
[9] T. Mattisson, H. Leion, A. Lyngfelt, Chemical-looping with oxygen uncoupling using CuO/ZrO2 with petroleum coke, Fuel 88 (2009) 683–690.
[10] J. Adanez, A. Abad, F. Garcia-Labiano, P. Gayan, L.F. de Diego, Progress in chemical-Looping combustion and reforming technologies, Progress in Energy and Combustion Science 38 (2012) 215–282.
[11] N. Berguerand, A. Lyngfelt, The use of petroleum coke as fuel in a 10 kWth chemical-looping combustor, International Journal of Greenhouse Gas Control 2 (2008) 169–179.
[12] T. Pröll, K. Mayer, J. Bolhàr-Nordenkampf, P. Kolbitsch, T. Mattisson, A. Lyngfelt, H. Hofbauer, Natural mineral as oxygen carriers for chemical looping combustion in a dual circulating fluidized bed system, Energy Procedia 1 (2009) 27–34.
[13] P. Kolbitsch, J. Bolhar-Nordenkampf, T. Pröll, H. Hofbauer, Comparison of two Ni-based oxygen carriers for chemical looping combustion of natural gas in 140 kW continuous looping operation, Industrial and Engineering Chemistry Research 48 (2009) 5542–5547.
[14] H. Leion, A. Lyngfelt, M. Johansson, E. Jerndal, T. Mattisson, The use of ilmenite as an oxygen carrier in chemical-looping combustion, Chemical Engineering Research and Design 86 (2008) 1017–1026.
[15] T. Pröll, P. Kolbitsch, J. Bolhar-Nordenkampf, H. Hofbauer, A novel dual circulating fluidized bed system for chemical looping processes, AIChE Journal 55 (2009) 3255–3266.
[16] H. Leion, T. Mattisson, A. Lyngfelt, Solid fuels in chemical-looping combustion, International Journal of Greenhouse Gas Control 2 (2008) 180–193.
[17] A. Lyngfelt, Oxygen carriers for chemical looping combustion-4000 h of operational experience, Oil and Gas Science and Technology 66 (2011) 161–172.
[18] M. Orth, J. Ströhle, B. Epple, Design and operation of a coal-fired 1 MWth chemical looping pilot plant, in: Proceedings of the 2nd International Conference of Chemical Looping, 2012.
[19] J. Adanez, A. Cuadrat, A. Abad, P. Gayan, L.F. de Diego, F. Garcia-Labiano, Ilmenite activation during consecutive redox cycles in chemical-looping combustionm, Energy and Fuels 24 (2010) 1402–1413.
[20] F. Li, Z. Sun, S. Luo, L.S. Fan, Ionic diffusion in the oxidation of iron-effect of support and its implications to chemical looping applications, Energy and Environmental Science 4 (2011) 876–880.
[21] M.M. Azis, E. Jerndal, H. Leion, T. Mattisson, A. Lyngfelt, On the evaluation of synthetic and natural ilmenite using syngas as fuel in chemical looping combustion (CLC), Chemical Engineering Research and Design 88 (2010) 1505–1514.
[22] Z.P. Gao, L.H. Shen, J. Xiao, M. Zheng, J.H. Wu, Analysis of reactivity of Fe-based oxygen carrier with coal during chemical-looping combustion, Journal of Fuel Chemistry and Technology 37 (2009) 513–520.
[23] M.N. Rahaman, Sintering of Ceramics, SRC Press, Boca Raton, Florida 45–176.
[24] F. Li, L. Zeng, L.G. Velazquez-Vargas, Z. Yoscovits, L.S. Fan, Syngas chemical looping gasification process: bench-scale studies and reactor simulations, AIChE Journal 56 (2010) 2186–2199.
[25] D. Sridhar, A. Tong, H. Kim, L. Zeng, F. Li, L.S. Fan, Syngas chemical looping process: design and construction of a 25 kWth subpilot unit, Energy and Fuels 26 (2012) 2292–2302.
[26] P.C. Chiu, Y. Ku, Chemical looping process—a novel technology for inherent CO_2 capture, Aerosol and Air Quality Research 12 (2012) 1421–1432.